Moroccan Journal of Chemistry
ISSN : 2351-812X

Mor. J. Chem., 2023, Volume 11, Issue 4, Page 965-978
https://revues.imist.ma/index.php/morjchem
https://doi.org/10.48317/IMIST.PRSM/morjchem-v11i04.40939

Preparation and Characterization of New Mixed Azo Ligand Complexes with Some Metal Ions and in Vitro Biological Activity and Molecular Docking Study of their Ni(II) and Hg(II) Complexes

Fatema Jabbar Ali[a], Esraa Rasool Radhi[a*], Afaq Jaber Kadhium[b], Khdeeja Jabbar Ali[b]

[a] *Ministry of Education, Kufa, Iraq,*
[b] *Chemistry Department, Education for Girls Faculty, Kufa University, Kufa, Iraq*
** Corresponding author email: esraarasul@gmail.com*

Received *13 June 2023,*
Revised *18 July 2023,*
Accepted *22 July 2023*

Citation*: Ali F. J., Radhi E. R., Kadhium A. J., Ali K. J. (2023) Preparation and Characterization of New Mixed Azo Ligand Complexes with Some Metal Ions and in Vitro Biological Activity and Molecular Docking Study of their Ni(II) and Hg(II) Complexes, Mor. J. Chem., 11(4), 965-978*

Abstract: New mixed azo imidazole ligand complexes of Ni(II), Cu(II), Cd(II) and Hg(II) were prepared using (E)-2-((4- chloro phenyl)diazenyl)-4,5-bis(4-methoxy phenyl)-1H-imidazole (CPDMI) as a primary ligand and (E)-2-((4- bromo phenyl)diazenyl)- 4,5-bis(4-methoxy phenyl)-1H-imidazole (BPDMI) as a secondary ligand, the general formula for all ions was $[M(L_1L_2Cl_2)].H_2O$. The prepared metal ion complexes were characterized by FT-IR, UV–Vis spectrophotometric, ^{1}H-NMR, mass spectral analysis, molar conductivity, and magnetic moment techniques. Based on the obtained data, the suggested molecular structure of all the metal complexes is octahedral geometry. The biological activity of the free ligands and their Ni(II) and Hg(II) complexes has also been studied. The molecular docking study was employed to predict and optimize the antibacterial outcomes, and a satisfactory concurrence between experimental and theoretical results was observed.

Keywords: Preparation and characterization, Mixed ligands, Azo imidazole complexes, In vitro biological activity, Molecular docking study.

1. Introduction

Mixed ligands contain at least two different functional groups that can bind to metallic ions to form complexes. Currently, there is increasing interest in the development of these compounds due to the different features connected with each atom conferring a characteristic reactivity to their complexes (Mahmoud & Ibraheem, 2014). Studying the coordination chemistry of mixed ligand complexes with transition metals is of current interest because they provide new compounds that have beneficial properties such as magnetic exchange (Mahmoud & Hassan, 2017), nonlinear optical properties (Modanawal *et al.*, 2021), photoluminescence (Mohamed *et al.*, 2006), and antimicrobial activity (Abebe *et al.*, 2017). Complexes of mixed ligands containing nitrogen and oxygen atoms as electron donors are significant compounds because of their antibacterial, antifungal and anticancer activities (habiban *et al.*, 2015). Mixed ligand complexes with transition metals are sometimes more effective in the biological field than the free ligands themselves (Youssef *et al.*, 2010). Mixed ligand complexes can act as active catalysts in hydrogenation and oxidation reactions (Bouhdada *et al.*, 2019).

Azo imidazole molecules contain the azoimine functional group (–N=N–C=N–), which is an effective π–acid system; therefore, these organic molecules form stable complexes with transition and non-transition metal ions (Mahdi & Ali, 2015; Mohammed *et al.*, 2013). Literature shows that imidazole compounds provided promising results against both Gram-positive and Gram-negative bacterial strains, thus further analysis should be performed in terms of toxicity, pharmacokinetics and pharmacodynamics. Additional screening of these imidazole derivatives could lead to useful compounds with potential broad-spectrum antibacterial activity against resistant pathogens (Valls *et al.*, 2020; Andrei *et al.*, 2021; Messali *et al.*, 2015; Saddik *et al.*, 2012).

Molecular docking is routinely used for the understanding of drug-receptor interaction. The "molecular docking" studies of all the heterocyclic derivatives against bacterial protein performed using the Molecular Operating Environment (MOE) and obtained conformations of ligand complexes and proteins were examined for binding energy and interactions of the docked structure (Koubi *et al.*, 2022; Xu *et al.*, 2023; Diass *et al.*, 2023; Sharma *et al.*, 2022).

In the present paper, two azo imidazole ligands and their mixed complexes with Ni(II), Cu(II), Cd(II) and Hg(II) were prepared and characterized by spectral and elemental analyses. The biological activity of both free azo ligands and their complexes with Ni(II) and Hg(II) was also examined. In addition to the theoretical study of molecular docking, it is crucial to examine the stability of the Ni(II) and Hg(II) complexes within the active site of the *E. coli* bacterium.

2. Materials and Methods

2. 1. Chemicals and Instruments

All the chemicals used were of analytical grade with high available purity except for the compound 4,5-bis(4-methoxy phenyl) imidazole, which was prepared as described in (Ali *et al.*, 2021). The melting point was determined by the Stuart-SMP10 melting point apparatus. The FT-IR spectra were recorded on a Shimadzu FT-IR 8400 spectrophotometer (KBr pellets). The ^{1}H-NMR spectra were recorded using a Brucker Biospin Gmph (500 MHz) spectrophotometer (DMSO-d6 as a solvent). The mass spectrum was obtained using a Shimadzu Agilent HP (5973). UV–Vis spectra were measured using a Shimadzu (UV-1700) spectrophotometer. Magnetic susceptibility was calculated by Sherwood Scientific balance magnetic susceptibility, and molar conductivity measurements were achieved by digital conductivity series ion. lab. 720.

2. 2. preparation of (E)-2-((4-chloro phenyl)diazenyl)-4,5-bis(4-methoxy phenyl)-1H-imidazole (CPDMI)

The CPDMI compound was prepared as described in (Ali *et al.*, 2021) by dissolving (1.275 g, 0.01 mol) 4-chloroaniline in a mixture of 20 mL of distilled water and 3 mL of concentrated HCl. Cool the resulting mixture to (0-5) ˚C and slowly add (0.70 g, 0.01 mol) of sodium nitrite dissolved in 10 mL of distilled water with continuous stirring and keeping the temperature at (0-5) ˚C. Let the solution settle for at least 30 minutes to complete the diazotization process. Mix the diazonium solution with (2.80 g, 0.01 mol) of 4,5-bis(4-methoxyphenyl) imidazole dissolved in a mixture solution containing 150 mL of ethanol with 5 mL of 10% sodium hydroxide. When the solution color was observed to change to red, the solution acidity was adjusted to 7 using drops of 0.1 N HCl and left for a day. The samples were filtered and washed with cold distilled water many times. Dried and recrystallized from ethanol. The CPDMI preparation steps are shown in **Scheme 1**.

2. 3. preparation of (E)-2-((4-bromo phenyl)diazenyl)-4,5-bis(4-methoxy phenyl)-1H-imidazole (BPDMI)

The BPDMI compound was prepared by dissolving (1.72 g, 0.01 mol) 4-bromoaniline in a mixture of 20 mL of distilled water and 3 mL of concentrated HCl. Cool the resulting mixture to (0-5) ˚C and slowly add (0.70 g, 0.01 mol) of sodium nitrite dissolved in 10 mL of distilled water with continuous stirring and keeping the temperature at (0-5) ˚C. Let the solution settle for at least 30 minutes to complete the diazotization process. Mix the diazonium solution with (2.80 g, 0.01 mol) of 4,5-bis(4-methoxyphenyl) imidazole dissolved in a mixture solution containing 150 mL of ethanol with 5 mL of 10% sodium hydroxide. When the solution color was observed to change to red, the solution acidity was adjusted to 7 using drops of 0.1 N HCl and left for a day. The samples were filtered and washed with cold distilled water many times. Dried and recrystallized from ethanol. The BPDMI preparation steps are shown in **Scheme 2**.

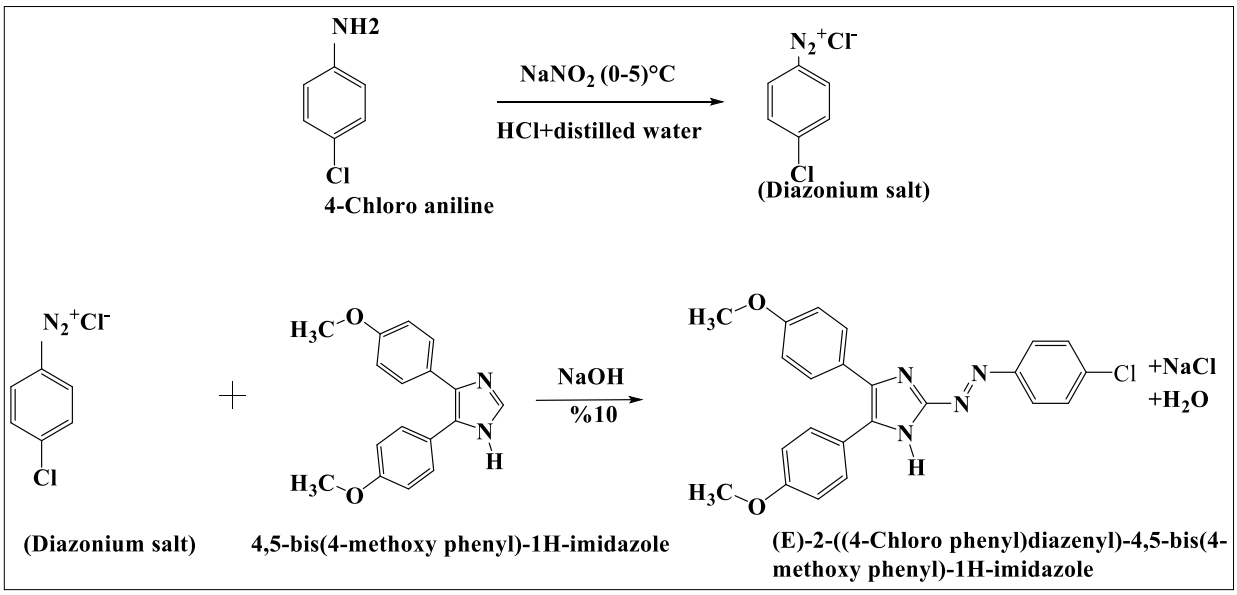

Scheme 1. The preparation steps of the ligand CPDMI

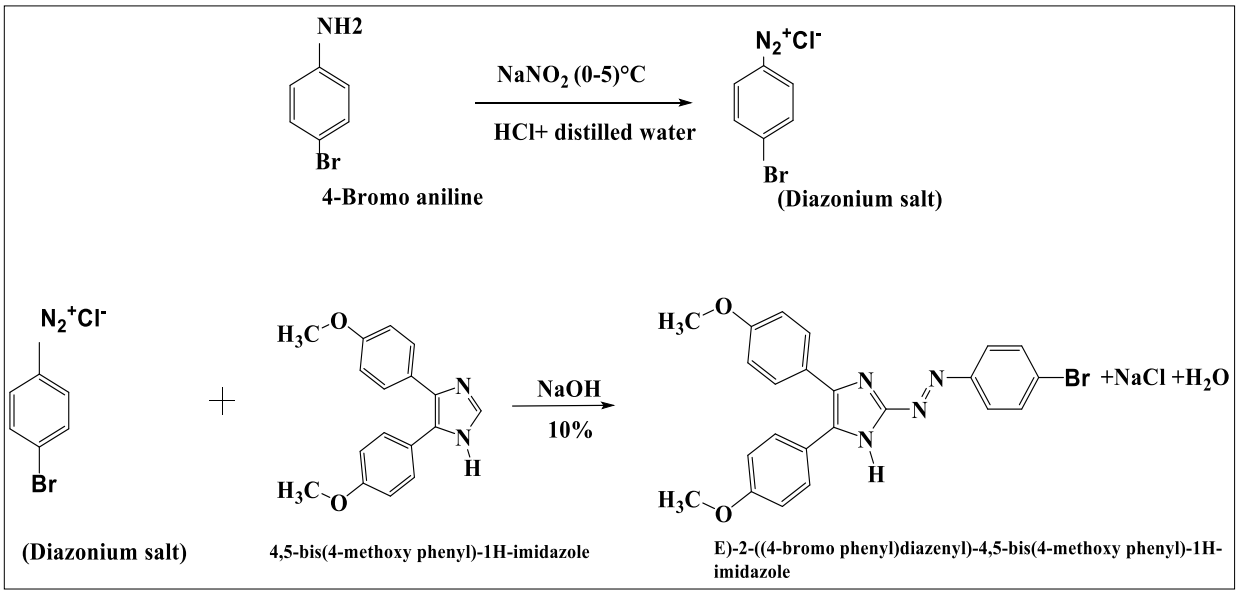

Scheme 2. The preparation steps of the ligand BPDMI

2. 4. Preparation of Mixed Azo Ligand Complexes

The mixed azo ligand complexes of Ni(II), Cu(II), Cd(II) and Hg(II) were prepared by mixing a solution of (0.418 g, 0.001 mol) CPDMI ligand dissolved in 75 mL ethanol, (0.463 g, 0.001 mol) BPDMI ligand dissolved in 75 mL ethanol, and an aqueous solution for the chloride salts of the above ions containing an appropriate weight of the specific ion dissolved in 5 mL distilled water to achieve the mole ratio (CPDMI:ion:BPDMI) (1:1:1). The resulting solutions were then refluxed at 70 °C for 90 minutes to complete the complexation reaction, allowed to cool to room temperature, filtered, washed with a mixture of 50% ethanol:water, and dried. **Table 1** shows some of the analytical properties of the prepared ligands and their complexes.

2. 5. Biological Activity Study

The antimicrobial activity of CPDMI, BPDMI and their mixed complexes with Ni(II) and Hg(II) was checked against two types of gram-positive bacteria (*Staphylococcus aureus* and *Enterococcus faecalis*) and two types of gram-negative bacteria (*Escherichia coli* and *Klebsiella pneumonia*). The study was performed by applying the agar well diffusion method. After the preparation of the agar medium, the chosen pathogens were swabbed along the solidified agar surface, followed by making wells in agar plates with a 6 mm diameter and then filling each well with 0.1 mL of the above compounds at increasing concentrations of 25, 50, 100, 200 and 400 µg mL^{-1}. The plates were then incubated at 37 °C for 24 hours. The biological activity was measured by calculating the inhibition zone in each plate.

Table 1. Analytical properties of CPDMI and BPDMI and their metal complexes

Chemical formula	Color	m.p °C	Yield %	M.f (M.wt)	Found % (Calc.)			
					C	H	N	M
CPDMI	Red	108	94	418.5	65.94	4.54	13.38	.....
$C_{23}H_{19}N_4O_2Cl$					(65.62)	(4.52)	(13.27)	.....
BPDMI	Red	104	90	463	59.611	4.103	12.095	.....
$C_{23}H_{19}N_4O_2Br$					(59.88)	(4.121)	(12.33)	.....
$[Cu(L_1L_2Cl_2)].H_2O$	Violet	245	88	1034.04	53.382	3.67	10.83	6.145
					(53.35)	(3.49)	(10.55)	(6.12)
$[Ni(L_1L_2Cl_2)].H_2O$	Violet	224	78	1029.19	53.63	3.69	10.88	5.702
					(53.55)	(3.45)	(10.36)	(5.70)
$[Cd(L_1L_2Cl_2)].H_2O$	Deeb-red	202	68	1082.9	50.974	3.509	10.34	10.37
					(50.92)	(3.47)	(10.32)	(10.36)
$[Hg(L_1L_2Cl_2)].H_2O$	Deeb-red	195	66	1171.09	47.135	3.244	9.563	17.128
					(47.132)	(3.221)	(9.54)	(17.40)

2. 6. Ligand preparation

The Molecular Operating Environment (MOE) software was utilized to screen the prepared azo ligands and their mixed complexes with Ni(II) and Hg(II). Gentamicin was used as an antibacterial control obtained from the PubChem database (http://pubchem.ncbi.nlm.nih.gov), their 3D structure was prepared in an SDF (structure-data file) format and selected to perform molecular docking studies. Two methods were employed for compound screening: (a) pharmacophore-based screening and (b) molecular docking. In the pharmacophore-based virtual screening, the Compute option of MOE was used to select the pharmacophoric features of the co-crystalized ligand, such as anionic and cationic

atoms, H-bond donors and acceptors, aromatic centers, Pi-ring centers, and hydrophobic centroids (Merzouki *et al.*, 2023). Once the ligand features were chosen, the software was executed to filter compounds based on these selected features in the co-crystal ligand. The resulting output file containing the compounds was then utilized for molecular docking.

2. 7. Molecular docking

In a molecular docking approach, the pharmacophore-based screened ligands were docked with the three-dimensional structure of the target protein. The study focused on the best result of biological activity using the protein structure of the *E. coli* bacteria (PDB ID: 1HNJ) **Figure 1**, obtained from the Research Collaboratory for Structural Bioinformatics (RCSB), and prepared in MOE for docking (Zazouli *et al.*, 2022). To predict the active site residues of the binding pocket, 3D protonation, energy minimization of the protein, and site finder were employed. Structure preparation included adding missing hydrogen atoms, correcting bond order assignments, adjusting charge states and orientations of various groups, and performing restrained minimizations that allowed hydrogen atoms to be freely minimized.

3. Results and Discussion

3. 1. Characterization of Free Ligands and their Metal Complexes

Both the prepared ligands, CPDMI and BPDMI, and their complexes are stable at room temperature, insoluble in water and fully soluble in methanol, ethanol, chloroform, and acetone. CPDMI and BPDMI ligands are red in color, while their prepared complexes have different colors depending on the coordinated ion. The measured magnetic susceptibilities of the prepared complexes were in agreement with the octahedral geometry for all the complexes. Spectral characterization by FT-IR, UV–Vis spectrophotometry, mass spectral analysis, and ^{1}H-NMR were performed for the prepared ligands and the complexes.

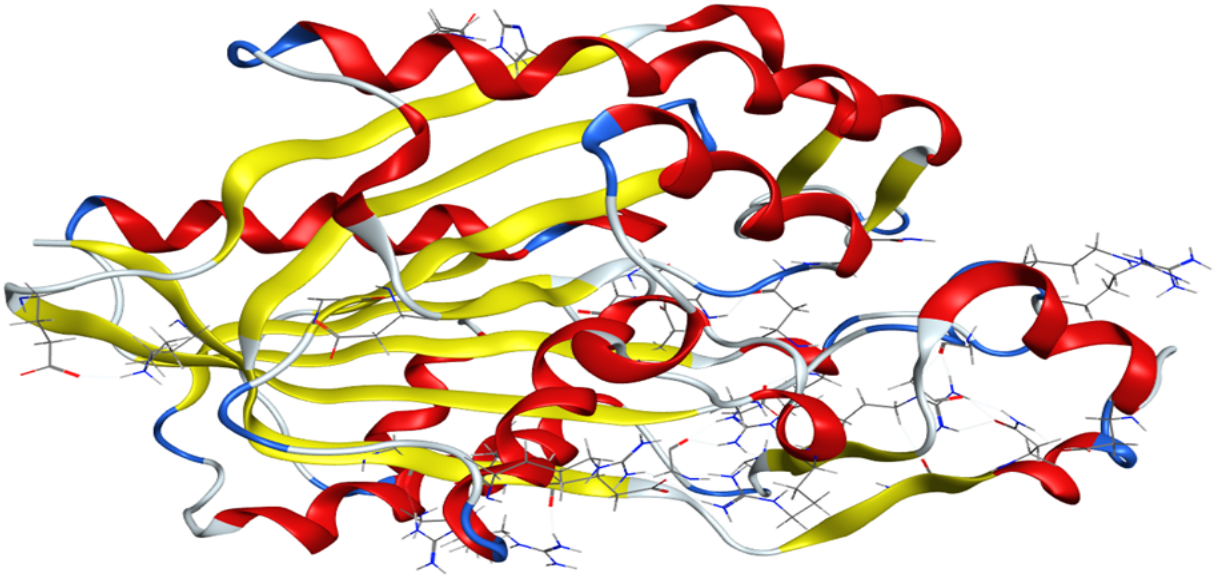

Figure 1. The three-dimensional structure of the *E. coli* protein.

3. 1. 1. Infrared Spectra of CPDMI, BPDMI and their Complexes

The FT-IR spectra of the free ligands exhibited stretching vibrations at 1639 and 1641 cm^{-1} for CPDMI and BPDMI, respectively, due to the (C=N) group of the imidazole molecule (Ali & Alabidi 2019; HUSSEIN & MAHDI 2019). This absorption frequency was shifted to lower frequencies (1608-

1610) cm^{-1} in the spectra of the complexes, confirming the participation of this group in complex formation with metal ions. The band at 788 cm^{-1} in the CPDMI free ligand spectra was assigned to the (C-Cl) group (Ali *et al.*, 2021), while the band at 605 cm^{-1} was assigned to the (C-Br) group in the BPDMI free ligand. The broad stretching vibration at 2835 cm^{-1} in all spectra is attributed to the etheric ($O-CH_3$) bond. The vibrations at (416-474) cm^{-1} in the spectra of the complexes can be attributed to the M-N bond (Jarad *et al.*, 2012). **Figure 2** shows the FT-IR spectra of CPDMI, BPDMI and the Cd-complex, and **Table 2** illustrates the infrared data of CPDMI, BPDMI**,** and their complexes.

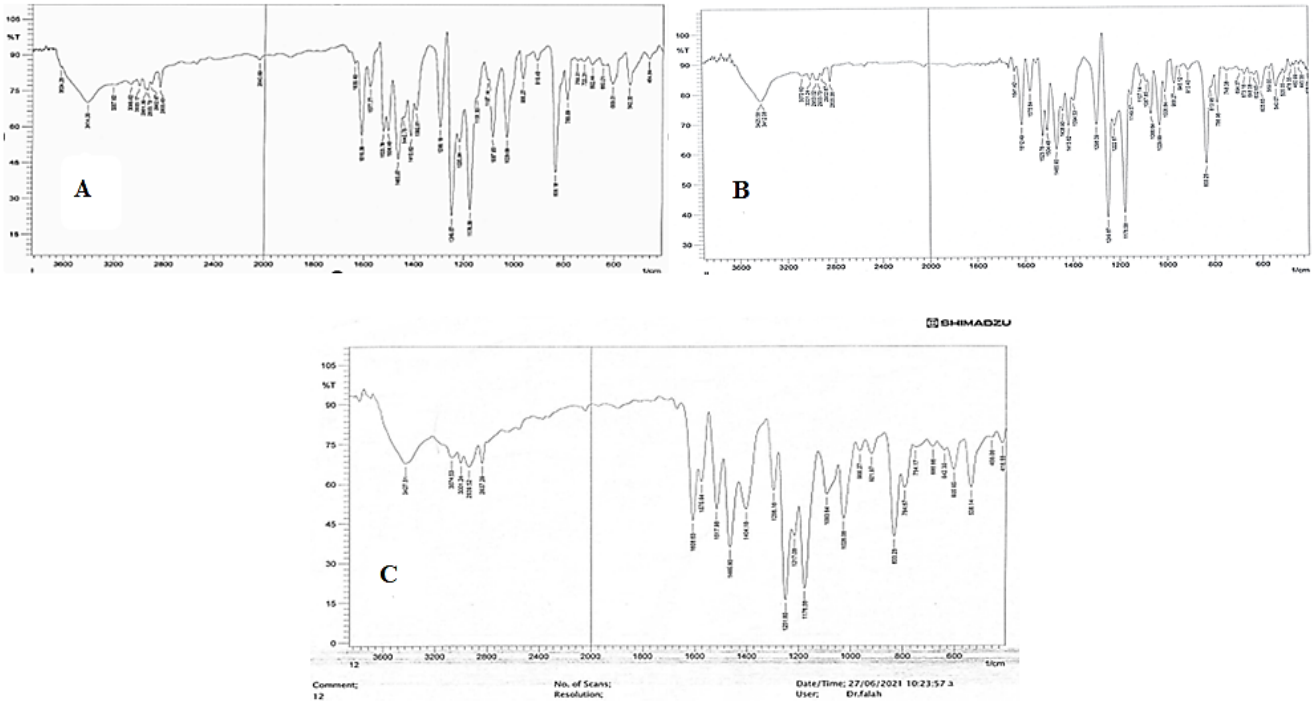

Figure 2. FT-IR spectra of **A**: CPDMI, **B**: BPDMI and **C**: Cd- complex

Table 2. Selected infrared vibrations (cm^{-1}) for CPDMI, BPDMI, and their complexes.

Compound	***ν* (N-H) + *ν* (O-H)**	**ν $(C-H)_{ar.}$**	***ν* $(C-H)_{al.}$**	***ν* (C=N)**	***ν* (N=N)**	***ν* (M–N)**
L_1 = CPDMI $C_{23}H_{19}N_4O_2CL$	3414 b.	3066 w.	2951 w.	1639 w.	1463 m.	-------
L_2 = BPDMI $C_{23}H_{19}N_4O_2Br$	3412 b.	3001 w.	2835 w.	1641 m.	1465 m.	-------
$[Cu(L_1L_2Cl_2)].H_2O$	3400 b.	3001 w.	2937 w.	1608 w.	1462 m.	474 w.
$[Ni(L_1L_2Cl_2)].H_2O$	3385 b.	3003 w.	2939 w.	1610 w.	1462 m.	460 w.
$[Cd(L_1L_2Cl_2)].H_2O$	3427 b.	3074 w.	2939 w.	1608 w.	1465 m.	418 w.
$[Hg(L_1L_2Cl_2)].H_2O$	3410 b.	3066 w.	2939 w.	1608 m.	1463 m.	416 w.

m.= medium, w.= weak, br.= broad, ar.= aromatic, al.=aliphatic.

3. 1. 2. Electronic Spectra of CPDMI, BPDMI and their Complexes

UV–VIS spectra of the free synthesized ligands and their Cd(II) mixed complex are shown in **Figures 3 and 4**, respectively. The spectra of both ligands showed main peaks at 21598 and 21739 cm^{-1} due to the electronic transition ($n \rightarrow \pi^*$) for CPDMI and BPDMI, respectively, while the main peak at 32362

cm^{-1} in the CPDMI and BPDMI spectra is due to the electronic transition ($\pi \rightarrow \pi^*$) (Gandioso *et al.*, 2015). The peaks in the spectra of the two ligands attributed to the internal charge transitions are shifted to higher wavelengths in the spectra of the complexes due to coordination with the transition ions (Kadhium & Abdulrasool, 2022). Cd(II) and Hg(II) complexes have saturated d orbitals (nd^{10}), so they do not show any d-d transitions; instead, they show charge transfer transitions (M→L, CT) (Kadhium *et al.*, 2019). The prepared complexes have different magnetic moment values with octahedral geometry (Sp^3d^2). The analytical data of CPDMI, BPDMI and their mixed complexes are shown in **Table 3**; the proposed structure of the synthesized mixed complexes is illustrated in **Scheme 3**.

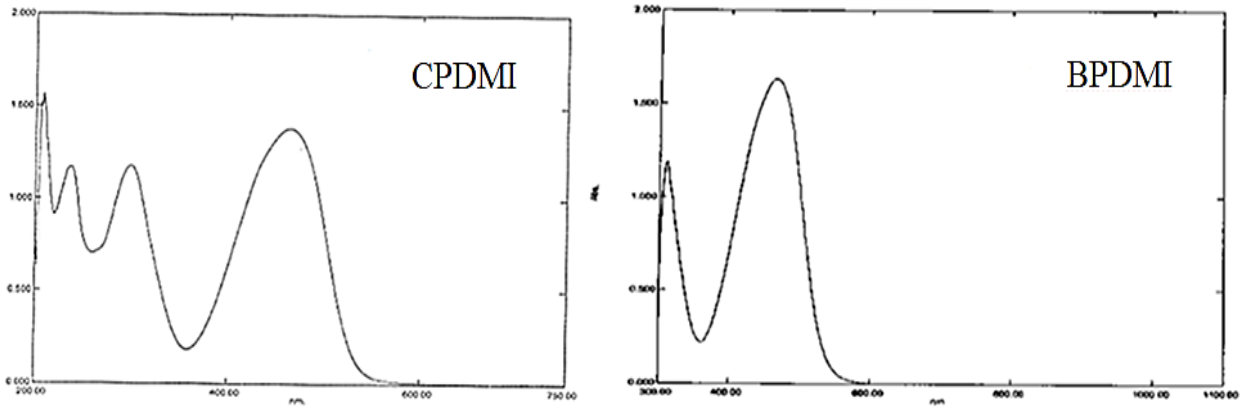

Figure 3. UV–VIS spectra of CPDMI and BPDMI free ligands

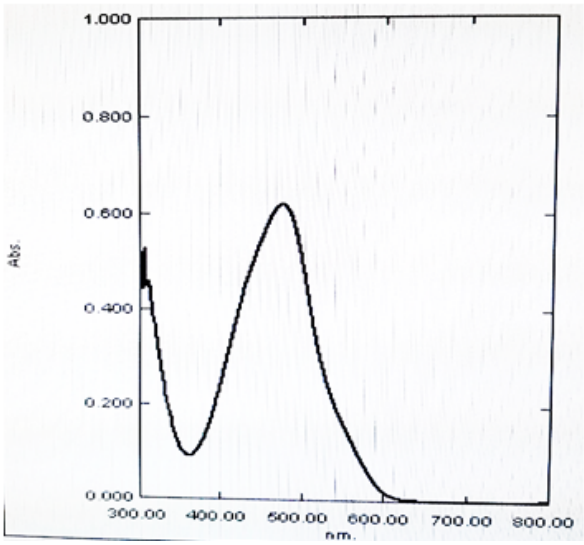

Figure 4. UV–VIS spectrum of $[Cd(L_1L_2Cl_2)].H_2O$ complex

3. 1. 3. ^{1}H-NMR Spectrum of $[Cd(L_1L_2Cl_2)].H_2O$

The ^{1}H-NMR spectrum of $[Cd(L_1L_2Cl_2)].H_2O$, as shown in **Figure 5**, shows a single signal at δ = 13.42 ppm attributed to the amine group's proton of the middle ring (Jarallah *et al.*, 2019; Karakus *et al.*, 2018). The multiplet signals at δ = 6.93-8.08 ppm were assigned to the aromatic protons (Xie *et al.*, 2018), whereas the signal at δ = 3.40 ppm was assigned to the methoxy protons in the imidazole molecule. Signals at δ = 3.80 ppm were attributed to the water molecule, while the signal at δ = 2.52 was assigned to the solvent protons.

Table 3. The analytical data of IPDHQ, BPDMI and their mixed complexes.

Compound	λ_{max} (nm)	Absorption Band (cm^{-1})	Transition	μ_{eff} (B.M)	Geometry	Hybridization
L_1 = CPDMI	463	21598	n →π*	.....	.....	.....
$C_{23}H_{19}N_4O_2CL$	309	32362	π →π*	.....	.....	.....
L_2 = BPDMI	460	21739	n →π*	.....	.....	.....
$C_{23}H_{19}N_4O_2CL$	309	32362	π →π*	.....	.....	.....
$[Cu(L_1L_2Cl_2)].H_2O$	535	18691	$^2E_g \rightarrow {}^2T_{2g}$	1.71	Octahedral	Sp^3d^2
$[Ni(L_1L_2Cl_2)].H_2O$	593	16863.41	$^2E_g \rightarrow {}^2T_{2g}$	1.81	Octahedral	Sp^3d^2
$[Cd(L_1L_2Cl_2)].H_2O$	475	21052	M→L,CT	Dia	Octahedral	Sp^3d^2
$[Hg(L_1L_2Cl_2)].H_2O$	593	16863.41	M→L,CT	Dia	Octahedral	Sp^3d^2

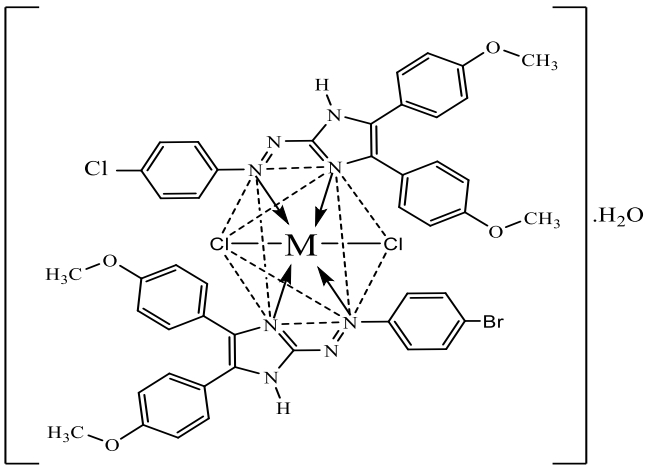

M= Ni(II), Cu(II), Cd(II), and Hg(II)

Scheme 3. The suggested structure of the mixed ligand complexes

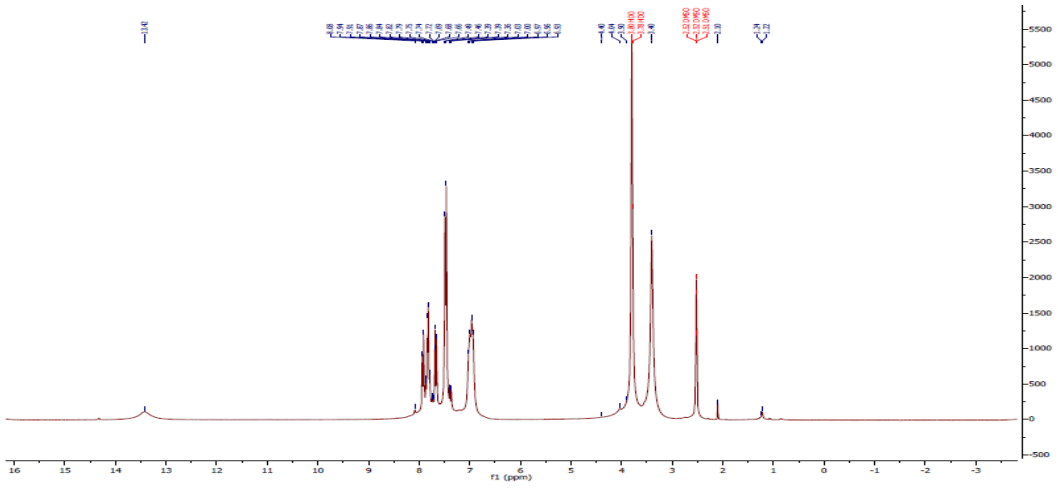

Figure 5. ^{1}H-NMR spectrum of $[Cd(L_1L_2Cl_2)].H_2O$

3. 1. 4. Mass Spectrum of $[Cd(L_1L_2Cl_2)].H_2O$

The mass spectrum of $[Cd(L_1L_2Cl_2)].H_2O$ showed a molecular ion peak at m/z^+ = 419.9 (40%) attributed to the main molecular weight of $[C_{23}H_{19}N_4O_2Cl]^+$ after gaining a proton, while the molecular peak appearing at m/z^+ = 463 (15%) was attributed to the free ligand $[C_{23}H_{19}N_4O_2Br]$. The peak at m/z^+ = 1082.9 (3%) is attributed to $[Cd(L_1L_2Cl_2)].H_2O$ complex. Several peaks assigned to the molecular

ions at m/z$^+$ = 280, 221, 77, and 69 were due to the fragment ions $[C_{17}H_{16}N_2O_2]^+$, $[C_{15}H_{13}N_2]^+$, $[C_6H_5]^+$, and $[C_3H_5N_2]^+$, respectively (Ali *et al.*, 2015). These data are in good agreement with the corresponding molecular formula of the complex, as shown in **Figure 6**.

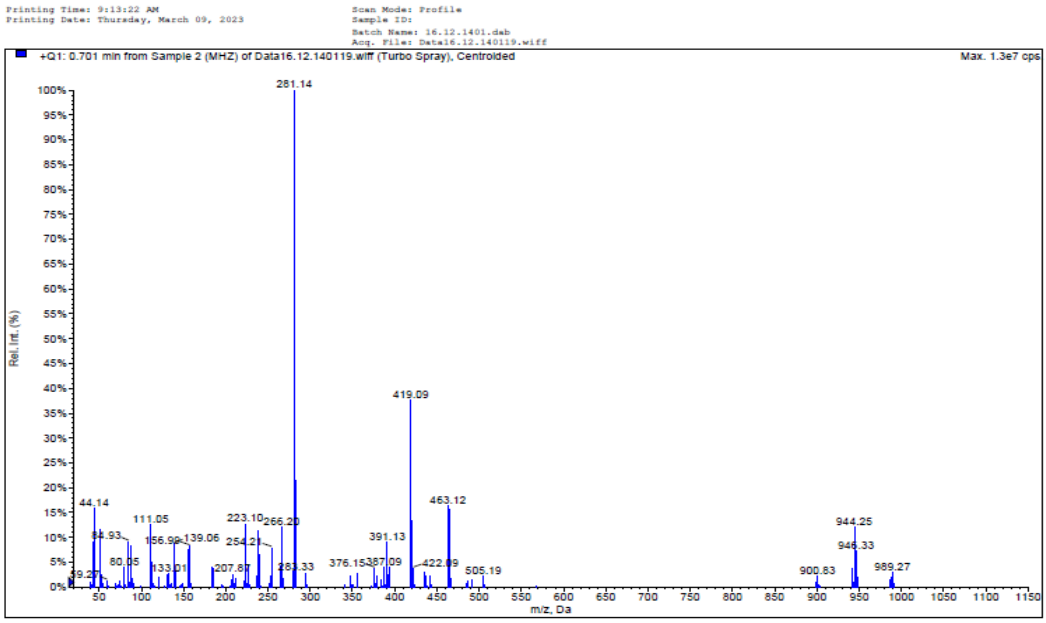

Figure 6. Mass spectrum of $[Cd(L_1L_2Cl_2)].H_2O$

3. 2. Biological Activity Study of CPDMI, BPDMI, and their Ni(II) and Hg(II) Complexes

The biological activity of the prepared azo ligands and their mixed complexes with Ni(II) and Hg(II) was studied against two types of gram-positive bacteria (*S. aureus* and *E. faecalis*) and two types of gram-negative bacteria (*E. coli* and *K. pneumoniae*) by applying the agar well diffusion method. The results listed in **Table 4** indicated that both free ligands exhibited approximately the same inhibition activity against all the bacterial types, with no inhibition activity at concentrations of 25 and 50 µg mL^{-1}. Both complexes exhibited higher inhibition activity than the free ligands. The Ni(II) complex showed higher activity against E. faecalis and E. coli bacteria than S. aureus and lower inhibition activity against *K. pneumonia*, while the Hg(II) complex showed higher inhibition activity against the two gram-negative bacteria types. At a concentration of 25 µg mL^{-1}, the two complexes did not exhibit any biological activity against any type of bacteria.

3.3. Molecular Docking Studies

The molecular docking approach is employed to simulate the atomic-level interaction between a small molecule and a protein, enabling the characterization of small molecule behavior within the binding site of target proteins and the elucidation of fundamental biochemical processes (Diass *et al.*, 2023). For the in silico docking study with a bacterial protein from E. coli, a comprehensive selection of Compounds, including both experimental compounds and control groups, was chosen. In the study, all ligands were successfully docked to the respective proteins using a molecular docking approach. The binding scores and hydrogen bond interactions of the ligand-protein complexes were evaluated and recorded in **Table 5**. The two-dimensional ligand-protein images clearly illustrate that all the compounds effectively penetrated the active binding site located within the protein's cavity. Subsequently **Figure 7**, docking simulations were performed specifically on the active site of the 1HNJ protein.

Table 4. Biological activity of CPDMI, BPDMI, and their Ni(II) and Hg(II) complexes

Compound	Concentration µg mL^{-1}	gram-positive bacteria		gram-negative bacteria	
		S. aureus	*E. faecalis*	*E. coli*	*K. pneumoniae*
CPDMI azo ligand	25	-	-	-	-
	50	-	-	-	-
	100	12	14	13	14
	200	15	15	15	16
	400	17	16	15	17
BPDMI azo ligand	25	-	-	-	-
	50	-	-	-	-
	100	13	14	13	13
	200	15	14	15	15
	400	17	15	16	17
Ni(II) complex	25	-	-	-	-
	50	11	11	10	11
	100	12	14	13	12
	200	15	17	16	15
	400	17	18	18	16
Hg(II) complex	25	-	-	-	-
	50	12	13	15	14
	100	14	15	16	16
	200	16	16	18	17
	400	18	17	20	19

Table 5. Molecular docking data represented in terms of binding scores in Kcal /mole for 1HNJ proteins with compounds

N^0	Compound	1HNJ		H-bonds	Bond Distance (Å)
		S[a] kcal/mole	RMSD_Refine [b]		
1	CPDMI azo ligand	-6.946	1.180	GLU218	2.72
2	BPDMI azo ligand	-6.828	1.007	GLU218	2.46
3	Ni(II) complex	-7.027	1.312	ASP87	3.2
4	Hg(II) complex	-7.248	1.082	Met352	3.52
				ARG355	3.04
				ARG219	2.52
5	Gentamicin	-6.463	1.541	ASP87	2.12
					2.52
					2.28
				ARG355	1.99

[a] S: The score of the compound that placement inside the protein binding pocket.
[b] RMSD_Refine: The root mean squared deviation value between the predicted pose and those of the crystal one after and before the refinement process, respectively.

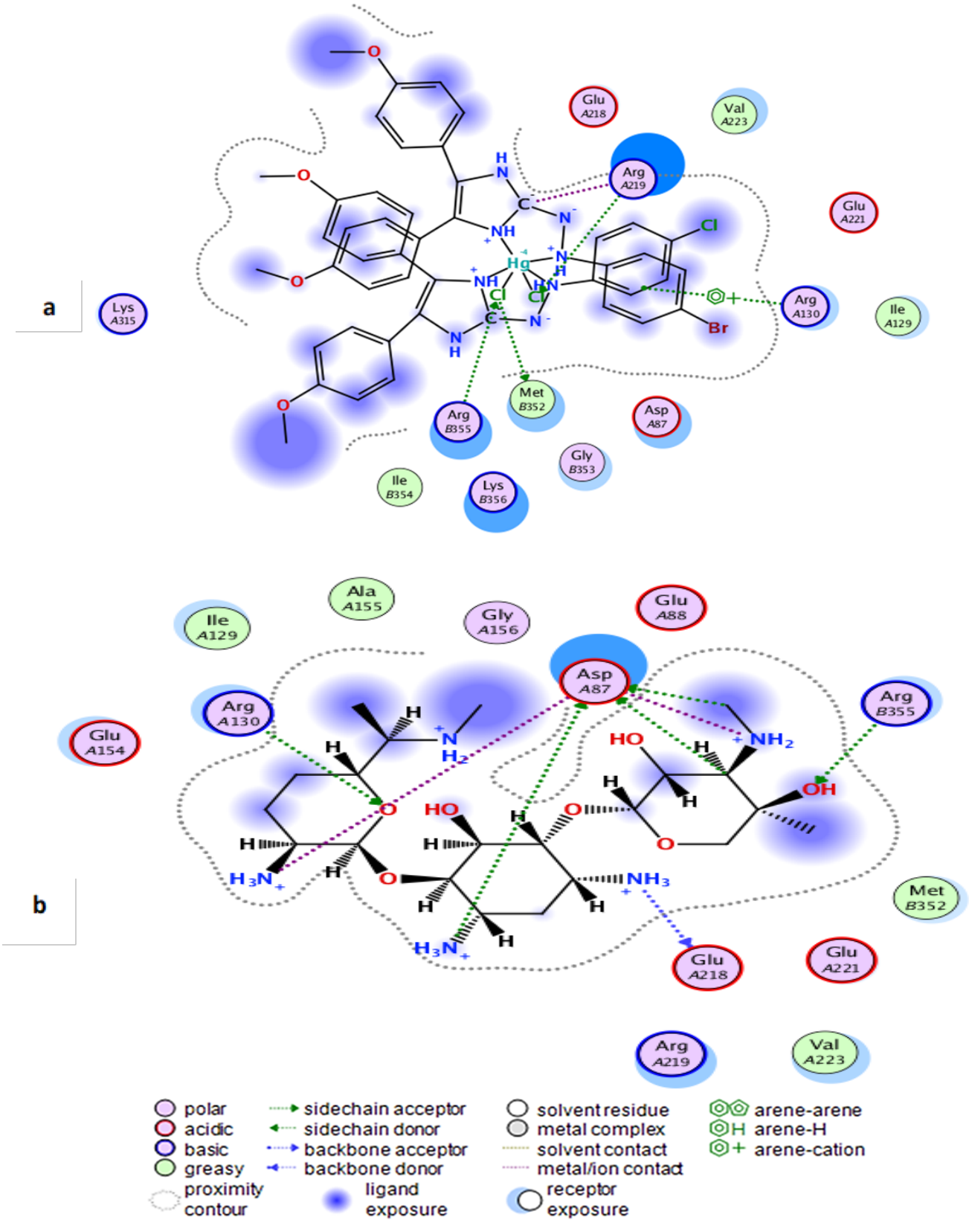

Figure 7. The 2D intermolecular interactions of the best result are depicted between (**a**) the Hg(II) complex and E. coli, and (**b**) the control compound Gentamicin with *E. coli*.

The results of these simulations indicated that all compounds exhibited higher binding energy values compared to gentamicin, which was utilized as the positive control in the experiment. This suggests

that the ligands have a stronger affinity for the protein than the reference compound. Moreover, the docking simulations provided insights into the stability of the ligands in the presence of Ni(II) and Hg(II) ions. The results demonstrated that the compounds exhibited greater stability when interacting with these metal ions compared to their stability when they were free ligands. This observation aligns with the findings from the biological activity study, which indicated that the compounds exhibited enhanced activity in the presence of Ni(II) and Hg (II) ions.

Conclusion

This work describes the preparation of two azo imidazole ligands and their mixed complexes with Ni(II), Cu(II), Cd(II), and Hg(II). The prepared azo ligands and their mixed complexes were characterized by various spectral and elemental analyses. Based on the obtained results, the proposed geometrical shape of all the prepared complexes was octahedral. The biological inhibition activity was tested for the two free ligands and their mixed complexes with Ni(II) and Hg(II) against four types of bacteria, and the results showed that all the compounds exhibited antimicrobial properties with higher inhibition activity for the Ni(II) and Hg(II) complexes than for the free ligands. In this study, the molecular docking approach proved to be a highly cost-effective method for identifying new targets for existing drugs. However, to confirm the therapeutic antibacterial properties of the Ni(II) and Hg(II) complexes, further laboratory and clinical investigations are necessary.

Disclosure statement: *Conflict of Interest:* The authors declare that there are no conflicts of interest.
Compliance with Ethical Standards: This article does not contain any studies involving human or animal subjects.

References

Abebe A., Sendek A., Ayalew S., & Kibret M. (2017) Copper(II) mixed-ligand complexes containing 1, 10-phenanthroline, adenine and thymine: Synthesis, characterization and antibacterial activities, *Chem. Int.*, 3(3), 230-239.

Ali, A. A. M., & Alabidi, H. M. (2019, September). Synthesis and Spectroscopic study of some transition metal complexes with 2-(4-Iodo Phenyl Azo)-4, 5-Diphenyl Imidazol. In Journal of Physics: Conference Series (Vol. 1294, No. 5, p. 052021). IOP Publishing. http://dx.doi.org/10.1088/1742-6596/1294/5/052021

Ali, A. A. M., Mohammed, H. J., & Khadhim, A. J. (2015). Preparation, Identification and Analytical Studies of the Ligand 2-[p-(2-pyrimidyl sulphamyI) phenylazo]-4, 5-diphenyl imidazole (PSPAI) and Some of its Metal Complexes. *IUG Journal of Natural Studies*, *16*(1).

Ali, F. J., AL-Ameri, L. A., & Ali, A. M. (2021). Synthesis and Identification and Biological Studies of New Azo Dyes Derived from Imidazole and their Chelate Complexes. *Indian J. Forensic Med. Toxicol.*, *15*(2), 1253-1260. https://doi.org/10.37506/ijfmt.v15i2.14496

Andrei G.Ș., Andrei B.F., & Roxana P.R. (2021) Imidazole Derivatives and their Antibacterial Activity-A Mini-Review. *Mini Rev. Med Chem.* 21(11), 1380-1392. https://doi.org/10.2174/1389557520999201209213648

Bouhdada, M., Amane, M. E., & El Hamzaoui, N. (2019). Synthesis, spectroscopic studies, X-ray powder diffraction data and antibacterial activity of mixed transition metal complexes with sulfonate azo dye, sulfamate and caffeine ligands. *Inorg. Chem. Commun.*, *101*, 32-39. http://dx.doi.org/10.1016/j.inoche.2019.01.005

Diass K., Oualdi I., Dalli M., Azizi S.-Ed, Mohamed M., Gseyra N., Touzani R., & Hammouti B. (2023) Artemisia herba alba Essential Oil: GC/MS analysis, antioxidant activities with

molecular docking on S protein of SARS-CoV-2, *Indonesian Journal of Science & Technology* 8(1), 1-18. http://dx.doi.org/10.17509/ijost.v8i1.50737

Gandioso, A., Shaili, E., Massaguer, A., Artigas, G., González-Cantó, A., Woods, J.A., Sadler, P.J., & Marchán, V. (2015). An integrin-targeted photoactivatable Pt (IV) complex as a selective anticancer pro-drug: synthesis and photoactivation studies. *Chemical Communications*, 51(44), 9169-9172. http://dx.doi.org/10.1039/C5CC03180J

Habiban, A. M., Mahmoud, W. A., & Kareem, T. A. (2015). Preparation and Characterization of Some Metal Complexes with Heterocyclic Azo Ligand (4-SuBAI). *Baghdad Science Journal*, *12*(3), 503-515.

Hussein, N. H., & Mahdi, R. T. (2019). Synthesis, Spectral characterization, Thermal analysis, Antimicrobial and Antitumor Properties of new azo ligand with some of its Transition Metal complexes. *Int. J. Pharm. Res.*, 11(1), 618-637.

Jarad, A. J., Kadhim, M. A., & Jabrallah, S. A. (2012). Synthesis and Spectral Studies of ZnII, CdII and HgII Complexes with 5-(2-Benzoic acid azo)-8-hydroxy quinoline Ligand. *Baghdad Science Journal*, 9(1), 178-186.

Jarallah, S. A., Nief, O. A., & Atia, A. J. K. (2019). Synthesis, characterization of heterocyclic compounds and preliminary evaluation of their antibacterial activity and antioxidant agents. *J. Pharm. Sci. Res.*, *11*(3), 1010-1015.

Kadhium, A. J., & Abdulrasool, R. N. (2022). Synthesis and characterization some transition metal complexes of new ligand chalcone-azo derivatives from P-methoxy-4, 5-diphenyl imidazole and study biological effect of Pd (II) complex. *NeuroQuantology*, 20(3), 173-181. http://dx.doi.org/10.14704/nq.2022.20.3.NQ22057

Kadhium, A. J., Mahdi, S. M., & Alrammahi, F. A. (2019). Preparation and Characterization of new Azo/Azo-Chalcone Ligands and their mixed ligands transition metal complexes with A study of Palladium Complex Anticancer Activity. *Res. J. Pharm. Technol.*, 12(12), 5947-5955. http://dx.doi.org/10.5958/0974-360X.2019.01032.

Karakus, M., Kara, I., Çelik, Ö., Orujalipoor, I., İde, S., & Yilmaz, H. (2018). Synthesis, characterization, single crystal structure and theoretical studies of trans-Ni (II)-complex with dithiophosphonate ligand. *Journal of Molecular Structure*, *1163*, 128-136. http://dx.doi.org/10.1016/j.molstruc.2018.02.110

Koubi Y., Hajji H., Moukhliss Y., El Khatabi K., El Masaoudy Y., Maghat H., Ajana M.A., Bouachrine M., & Lakhlifi T. (2022) in silico studies of 1,4-disubstituted 1,2,3-triazole with amide functionality antimicrobial evaluation against Escherichia coli using 3D-QSAR, molecular docking, and ADMET properties, *Mor. J. Chem.* 10, 689-702, https://doi.org/10.48317/IMIST.PRSM/morjchem-v10i4.34292

Mahdi, S. M., & Ali, A. M. (2015). Preparation &identification of new azo-schiff ligand with its complexes. *Iraqi Natl. J. Chem.*, *15*(2), 214-236.

Mahmoud W. A., & Ibraheem I. H. (2014) Synthesis and Spectral Analysis of Mn (II), Cu (II) ,Ni (II) and Cd (II) Complexes with Mixed Ligands containing 1,10-phenanthroline and Schiff base derived of 4-aminoantipyrine, *Baghdad Science Journal*, 11(4), 1519-1527. http://dx.doi.org/10.21123/bsj.11.4.1519-1527

Mahmoud, W. A., & Hassan, Z. M. (2017). Synthesis and spectral analysis of some metal ions complexes with mixed ligands of Schiff base and 1, 10-phenanthroline. *Baghdad Science Journal*, *14*(1), 0135-0135. http://dx.doi.org/10.21123/bsj.14.1.135-147

Merzouki M., Challioui A., Bourassi L., Abidi R., Bouammli B., El Farh L. (2023) In silico evaluation of antiviral activity of flavone derivatives and commercial drugs against SARS-CoV-2 main protease (3CLpro). *Mor. J. Chem.*, 11, 129-143. doi:10.48317/IMIST.PRSM/morjchem-v11i1.35278

Messali, M., Aouad, M. R., Ali, A. A. S., Rezki, N., Ben Hadda, T., & Hammouti, B. (2015). Synthesis, characterization, and POM analysis of novel bioactive imidazolium-based ionic liquids. *Med. Chem. Res.*, *24*, 1387-1395. http://dx.doi.org/10.1007/s00044-014-1211-x

Modanawal, V. K., Paswan, S., Anjum, A., Kumar, M., Srivastava, S., & Jaiswal, N. (2021). Synthesis, spectroscopic characterization, computational studies, theoretical investigation of NLO properties and antibacterial activities of mixed ligand complexes of Co (II) and Cu (II). *J. Coord. Chem.*, *74*(21-24), 3140-3152. http://dx.doi.org/10.1080/00958972.2021.2022128

Mohamed G. G., Omer M. M., & Hindy A. M. (2006) Metal Complexes of Schiff Bases: Preparation, Characterization, and Biological Activity, *Turk. J. Chem.*, 30(3), 361-382.

Mohammed, Z., Al-Khafagy, A. H., & Ali, A. M. (2013). Preparation, Characterization and Biological study of hetrocyclic Azo-Schiff Base compound and some of it's metal complexes. *Int. of J. of current Res*, *5*(12), 3705-3710.

Saddik, R., Khoutoul, M., Benchat, N., Hammouti, B., El Kadiri, S., & Touzani, R. (2012). Evaluation of catalytic activity of imidazolo [1, 2-a] pyridine derivatives: oxidation of catechol. *Res. Chem. Intermed.*, *38*, 2457-2470. http://dx.doi.org/10.1007/s11164-012-0561-6

Sharma A. D., & Kaur I. (2022) A novel therapeutic eucalyptol from eucalyptus essential oil targeting penicillin binding proteins (PBPs) against gram-positive and gram-negative bacteria: molecular docking and experimental approach, *Arabian Journal of Medicinal and Aromatic Plants,* 8(3), 24-42

Valls A., Andreu J.J., Falomir E., Luis S.V., Atrián-Blasco E., Mitchell S.G., & Altava B. (2020) Imidazole and Imidazolium Antibacterial Drugs Derived from Amino Acids. *Pharmaceuticals.* 13(12):482. https://doi.org/10.3390/ph13120482

Xie, W., Wu, Y., Zhang, J., Mei, Q., Zhang, Y., Zhu, N., Liu, R., & Zhang, H. (2018). Design, synthesis and biological evaluations of novel pyridone-thiazole hybrid molecules as antitumor agents. *Eur. J. Med. Chem.*, *145*, pp.35-40. http://dx.doi.org/10.1016/j.ejmech.2017.12.038

Xu W-B., Meng Y-Q., Sun J., Yang Y-X., Li W.-X., Wang M-Y., Piao M-G., Siqi Li, Quan J., & Jin C-H. (2023) Synthesis and Antibacterial Activity Evaluation of Imidazole Derivatives Containing 6-Methylpyridine Moiety, *Chem. Biodiversity*, 20(5), e202300105 https://doi.org/10.1002/cbdv.202300105

Youssef, N.S., El Zahany, E.A. & Ali, M.M., (2010). Synthesis, spectral, characterization, and anticancer activity of some binary and mixed ligand complexes of 4-methyl-2-pentanone thiosemicarbazone and some amino acids. *Phosphorus, Sulfur, and Silicon and the Related Elements*, *185*(11), pp.2171-2181. https://doi.org/10.1080/10426500903241739

Zazouli S., Chigr M., Atmani H., Jouaiti A. (2022). Synthesis, spectroscopic characterization of new series of alizarin derivatives and their anti-microbial activities: DFT and molecular docking approach. *J. Mol. Struct.*, 1256, 132527. https://doi.org/10.1016/j.molstruc.2022.132527